Kinetics of the Hydrogen Abstraction $^{\bullet}CH_3$ + Alkane → CH_4 + Alkyl Reaction Class: An Application of the Reaction Class Transition State Theory

Nawee Kungwan and Thanh N. Truong*

Henry Eyring Center for Theoretical Chemistry, Department of Chemistry, University of Utah, 315 South 1400 East, Room 2020, Salt Lake City, Utah 84112

Received: April 7, 2005; In Final Form: July 6, 2005

Kinetics of the hydrogen abstraction reaction $^{\bullet}CH_3 + CH_4 \rightarrow CH_4 + {}^{\bullet}CH_3$ is studied by a direct dynamics method. Thermal rate constants in the temperature range of 300−2500 K are evaluated by the canonical variational transition state theory (CVT) incorporating corrections from tunneling using the multidimensional semiclassical small-curvature tunneling (SCT) method and from the hindered rotations. These results are used in conjunction with the Reaction Class Transition State Theory/Linear Energy Relationship (RC-TST/LER) to predict thermal rate constants of any reaction in the hydrogen abstraction class of $^{\bullet}CH_3$ + alkanes. Our analyses indicate that less than 40% systematic errors on the average exist in the predicted rate constants using the RC-TST/LER method while comparing to explicit rate calculations the differences are less than 100% or a factor of 2 on the average.

1. Introduction

Reactions of methyl radicals with alkanes, $CH_3 + RH \rightarrow CH_4 + R$, play a significant role in the combustion process of hydrocarbons. At high temperatures large alkyl radicals degrade rapidly into the methyl radicals, which can be the primary chain carriers in thermal decomposition of hydrocarbons. The fate of the methyl radical is, however, not well characterized since the rate coefficients for their reactions with many hydrocarbons, such as C_nH_{2n+2}, are not known. Despite its importance, there are only about 10 such elementary reactions of this type where some experimental values are available. Yet there are only one to two of these reactions where such values are provided with some level of accuracy.[1] Theoretically, kinetics information is available only for reactions with methane[2,3] and ethane.[4]

The objective of the present study is to provide kinetic information for the hydrogen abstraction of alkanes by methyl radical using the Reaction Class Transition State Theory with Linear Energy Relationship (RC-TST/LER) method.[5,6] The RC-TST/LER theory provides an effective methodology for estimating thermal rate constants of all reactions in the class. The method is based on the idea that all reactions in a given class have the same reactive moiety and thus they are expected to have similar features on their potential surfaces along the specific reaction coordinate. The RC-TST explores such similarities so that they can be transferred from one reaction to another without having to explicitly calculate them. We found that it is possible to determine rate constants of any reaction in the class from that of a reference reaction, which is often the smallest reaction in the class, denoted as the principal reaction of that class, and a relative rate scaling factor expression that applies for the whole class. Furthermore, we have shown that within a given reaction class there is a linear energy relationship (LER)[6] similar to the Evans−Polanyi linear free-energy relationship between the classical barrier heights and reaction energies. Consequently, rate constants for any reaction can be predicted from just its reaction energy once all of the reaction class relative rate expressions are determined. Determining these expressions is the goal of this study. To do so, we selected a representative set of reactions in this class then performed explicit rate calculations. Detailed analyses of the relative rates of these reactions allow general expressions for relative rates for the entire class to be determined.

Hydrogen abstraction reactions of CH_3 with 16 different alkanes were used for determining the RC-TST/LER relative rate expressions. All of these reactions belong to the same reaction class given below:

$$^{\bullet}CH_3 + \text{alkane} \rightarrow CH_4 + \text{alkyl}$$

$$CH_3 + CH_4 \rightarrow CH_4 + CH_3 \quad \text{(R1)}$$

$$CH_3 + C_2H_6 \rightarrow CH_4 + C_2H_5 \quad \text{(R2)}$$

$$CH_3 + C_3H_8 \rightarrow CH_4 + n\text{-}C_3H_7 \quad \text{(R3)}$$

$$\rightarrow CH_4 + s\text{-}C_3H_7 \quad \text{(R4)}$$

$$CH_3 + C_4H_{10} \rightarrow CH_4 + n\text{-}C_4H_9 \quad \text{(R5)}$$

$$\rightarrow CH_4 + s\text{-}C_4H_9 \quad \text{(R6)}$$

$$CH_3 + (CH_3)_3CH \rightarrow CH_4 + (CH_3)_2CHCH_2 \quad \text{(R7)}$$

$$\rightarrow CH_4 + (CH_3)_3C \quad \text{(R8)}$$

$$CH_3 + n\text{-}C_5H_{12} \rightarrow CH_4 + 1\text{-}C_5H_{11} \quad \text{(R9)}$$

$$\rightarrow CH_4 + 2\text{-}C_5H_{11} \quad \text{(R10)}$$

$$\rightarrow CH_4 + 3\text{-}C_5H_{11} \quad \text{(R11)}$$

$$CH_3 + \text{neo-}C_5H_{12} \rightarrow CH_4 + (CH_3)_3\,CCH_2 \quad \text{(R12)}$$

$$CH_3 + \text{iso-}C_5H_{12} \rightarrow CH_4 + CH_2CH_2CH(CH_3)_2 \quad \text{(R13)}$$

$$\rightarrow CH_4 + CH_3CHCH(CH_3)_2 \quad \text{(R14)}$$

$$\rightarrow CH_4 + CH_3CH_2C(CH_3)_2 \quad \text{(R15)}$$

$$\rightarrow CH_4 + CH_3CH_2CH(CH_3)CH_2 \quad \text{(R16)}$$

* Address correspondence to this author. E-mail: truong@chem.utah.edu.

10.1021/jp051799+ CCC: $30.25
Published on Web 08/05/2005

These reactions represent hydrogen abstractions from the primary, secondary, and tertiary carbons.

Application of the RC-TST/LER method requires accurate rate constants of a reference reaction. Often the reference reaction is chosen to be the smallest one, i.e., the principal $CH_3 + CH_4$ reaction in this case. To the best of our knowledge, only two experimental[7,8] and one theoretical[3] studies on kinetics of this reaction have been reported. Due to the difficulty of detection and quantitatively measuring the product or reactant concentrations, there has been no direct measurement of the rate constants. Both experimental studies provide only relative or derived rate. In particular, one study derived the relative rate using the low flow and direct photolysis technique by employing the photolysis of acetone whose mechanism is well understood[9] and the other derived the relative rate from the detailed kinetics data for hydrogen abstraction from silane in the gas phase. The one theoretical study employed conventional Transition State Theory with a one-dimensional Eckart tunneling correction for a limited range of temperature. It has been known that for hydrogen abstraction by a radical of the H-L-H (heavy-light-heavy) type such as this reaction, tunneling is rather significant. Furthermore, the internal rotations of the two methyl groups at the transition state have not been treated explicitly previously. Thus, more accurate calculations for the thermal rate constants for the principal $CH_3 + CH_4$ reaction are also needed. In this study, we have carried out canonical variational TST calculations augmented by the multidimensional semiclassical small curvature tunneling corrections. Internal rotations of the two methyl groups at the transition state are treated as hindered rotors.

2. Methodology

Reaction Class Transition State Theory (RC-TST). Since the RC-TST/LER method has been described in detail in our previous reports,[5,6] we highlight only its main features here. Within the RC-TST framework, the rate constant of a target reaction (denoted as R_t) in a given reaction class, $k_t(T)$, is proportional to the rate constant of the reference reaction, for instance of the principal reaction (denoted as R_p) of the class, $k_p(T)$, by a temperature-dependent relative rate function $f(T)$:

$$k_t(T) = f(T)k_p(T) \tag{1}$$

The key idea of the RC-TST method is to factor $f(T)$ into different components:

$$f(T) = f_\kappa f_\sigma f_Q f_V \tag{2}$$

where, f_κ, f_σ, f_Q, and f_V are tunneling, symmetry number, partition function, and potential energy factors, respectively. These factors are simply the ratio of the corresponding components in the well-known TST expression (see eq 3) for two reactions:

$$f_\kappa(T) = \frac{\kappa_t(T)}{\kappa_p(T)} \tag{3}$$

$$f_\sigma = \frac{\sigma_t}{\sigma_p} \tag{4}$$

$$f_Q(T) = \left(\frac{Q_t^{\neq}(T)}{\Phi_t^{R}(T)}\right)\Big/\left(\frac{Q_p^{\neq}(T)}{\Phi_p^{R}(T)}\right) = \left(\frac{Q_t^{\neq}(T)}{Q_p^{\neq}(T)}\right)\Big/\left(\frac{\Phi_t^{R}(T)}{\Phi_p^{R}(T)}\right) \tag{5}$$

where Φ^R is the total partition function (per unit volume) of the reactants.

$$f_V(T) = \exp\left[-\frac{(\Delta V_t^{\neq} - \Delta V_p^{\neq})}{k_B T}\right] = \exp\left[-\frac{\Delta\Delta V^{\neq}}{k_B T}\right] \tag{6}$$

The principal task is to determine general expressions for these factors linking the rate constants of R_p and those of R_t in the same class without having to calculate $k_t(T)$ explicitly. This is done by performing explicit rate determinations for the above representative set of reactions using the TST method with the one-dimensional Eckart tunneling approximation then analyzing the "exact" calculated relative rate factors as functions of temperature to derive general expressions for the whole class. The rational for using the TST/Eckart method for this purpose has been discussed previously.[5,6] The calculated barrier heights and reaction energies for the above representative set of reactions also allow us to determine the LER between them that also can be used for the entire class.

Electronic Structure Calculations. All the electronic structure calculations were performed using the G98 program.[10] The geometries and harmonic vibrational frequencies of all the stationary points for all reactions listed above (the reactants, transition state, and products) were calculated at the hybrid BH&HLYP level of density functional theory with the cc-pVDZ basis set. The BH&HLYP method has been found previously to be sufficiently accurate for predicting the transition state properties for hydrogen abstraction reactions by radical.[11−13] In addition, the minimum energy path (MEP) of the principal $CH_3 + CH_4$ reaction was obtained using the Gonzalez−Schlegel method[14] in the mass-weighted Cartesian coordinates with a step size of 0.01 $(amu)^{1/2}$ bohr. Moreover the reaction barrier heights of all reactions were further refined using the IMOMO approach[15−17] within the reaction class framework at the CCSD(T)/cc-pVTZ:BH&HLYP/cc-pVDZ level of theory. In addition, for the principal reaction, harmonic vibrational frequencies were calculated at 20 selected points (10 points in the reactant channel, 10 points in the product channel) along the MEP. However, since the MEP is symmetric, actual calculations were only done for 10 points on the reactant side.

Thermal rate constants in the temperature range of 300−2500 K were calculated for all reactions using our web-based kinetics module within the Computational Science and Engineering Online suite.[18] For the principal reaction, rate constants were also calculated using the canonical variational transition state theory (CVT) augmented with the multidimensional semiclassical small-curvature tunneling (SCT) method[19] and hindered rotor treatment[20] for rotations of the two methyl groups in the transition state region. For comparison purposes, the zero-curvature tunneling (ZCT) method was also employed. To develop the RC-TST/LER parameters, rate constants of all listed reactions including the reference reactions were calculated using the TST method with one-dimensional Eckart tunneling corrections. The hindered rotation treatment was included explicitly in the rate constants of the reference reaction.

3. Results and Discussion

3.1. $^{\bullet}CH_3 + CH_4 \rightarrow CH_4 + {}^{\bullet}CH_3$ Reaction. *Stationary Points.* The optimized geometrical parameters of the reactants and products (CH_3 and CH_4) at the BH&HLYP/cc-pVDZ level of theory are shown in Figure 1. The transition state (TS) was found to have D_{3d} symmetry. Its geometrical parameters are given in Figure 1 and Table 1. The TS was confirmed by normal-mode analysis to have only one imaginary frequency whose mode corresponds to the transfer of the hydrogen atom. From Figure 1 and Table 1, both B3LYP and BH&HLYP optimized TS geometries are in excellent agreement with that

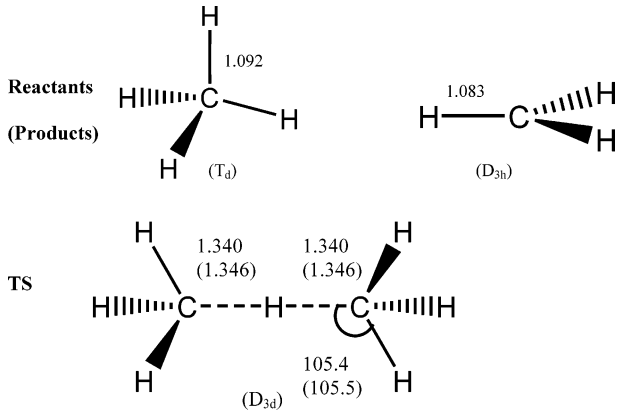

Figure 1. Optimized geometrical parameters (in angstroms and degrees) of the stationary points at the BHandHLYP/cc-pVDZ. The numbers in parentheses are optimized at the QCISD/cc-pVDZ level.

from the QCISD level calculations using the same basis set. We found that at the transition-state structure a low-frequency vibration at about 43 cm^{-1} from the BH&HLYP level of theory corresponds to the internal rotation around the 3-fold rotational axis. This indicates that the potential energy along this direction is relatively flat and thus harmonic approximation may not be accurate in calculating its partition function, hence a hindered rotor treatment is required in its rate calculations. Furthermore, the BH&HLYP imaginary frequency at the saddle point of 1884*i* cm^{-1} agrees much better with the QCISD result of 1923*i* cm^{-1} than with the B3LYP value of 1657*i* cm^{-1}. The imaginary frequency often correlates the width of the barrier and has a significant role in the tunneling dynamics. The potential barriers with ZPE corrections calculated at various levels of theory are listed in Table 2. It is interesting to note that accurate levels of theory such as G2, CCSD(T), QCISD, and PMP4 predict the barrier between 18 and 19 kcal/mol. The BH&HLYP value of 17.4 kcal/mol is lower but quite close to this range compared to 14.6 kcal/mol from the more widely employed B3LYP method. This is in fact consistent with the previous finding that the B3LYP method underestimates the barrier for hydrogen abstraction reactions while the BH&HLYP performs well for transition state properties in comparison to more accurate results.[11−13]

Minimum Energy Path. The minimum energy path (MEP) of the principal reaction was calculated at the BH&HLYP/cc-pVDZ level. The classical potential energy $V_{mep}(s)$, the ground-state adiabatic potential energy $V_a^G(s)$, and the zero-point energy ZPE(s) as functions of the reaction coordinate (s) are shown in Figure 2a, where $V_a^G(s) = V_{mep}(s) + \mathrm{ZPE}(s)$. The total ZPE curve has a small drop prior to the saddle point zone due to the decrease in the frequency of the reactive mode in this region, as discussed in more detail below. In fact, ZPE correction has lowered the barrier by 0.3 kcal/mol. We found that the $V_{mep}(s)$ and $V_a^G(s)$ curves are similar in shape. Figure 2b shows the changes of the bond distances along the reaction coordinate. As the reaction proceeds from the entrance channel, the breaking C−H′ bond length remains fairly constant until s reaches −0.5 $(amu)^{1/2}$ bohr then it steadily increases. Symmetrically, the forming bond decreases until $s = 0.5$ $(amu)^{1/2}$ bohr then remains constant. This indicates that the hydrogen abstraction process occurs at $-0.5 < s < 0.5$ or in the top 6 kcal/mol of the barrier. The first 12 kcal/mol of the barrier is mostly due to the repulsion interaction between the methyl radical and methane. This observation is further supported by the generalized vibration frequencies along the reaction coordinate as shown in Figure 2c. The largest variation in the generalized frequencies is seen at $-0.5 < s < 0.5$. In particular, the active C−H bond shows a sharp drop in its C−H stretching frequency starting at s about −0.5 then starts to increase after passing the saddle point indicating the new C−H bond is forming. Note that the active C−H stretching mode does not show a smooth curve in this region because the normal modes are not correlated as functions of the reaction coordinate. Such a correlation assumes that the generalized vibrational modes preserve their characteristic motions along the reaction coordinate. Correlation of the generalized normal modes is not needed for rate calculations and thus was not done here.

Rate Constants. The rate constants of the forward reactions are calculated using the canonical variational transition state theory (CVT) with the SCT, ZCT, and hindered rotor corrections over a wide temperature range from 300 to 2500 K. Geometries and vibrational frequencies at the BH&HLYP level were used. The potential energy along the reaction coordinate was scaled uniformly to match the barrier of 18.1 kcal/mol as predicted from the more accurate CCSD(T) level of theory. The internal rotation of the methyl groups about the D_{3d} rotational axis is treated using the hindered rotor treatment suggested by Ayala et al.[21] It is important to point out that even though this reaction is symmetric, the temperature-dependent dynamical bottleneck, i.e., the variational TS, is not necessarily located at the TS, i.e., $s = 0.0$, since the entropic contribution to the free energy increases as the reaction proceeds from the TS to the product or reactant channel. Thus, for accounting for the re-crossing effects, the variational treatment is still needed here. Furthermore, for SCT and ZCT tunneling calculations potential energy surface information along the MEP is required.

The calculated results along with available experimental data are listed in Table 3. An Arrhenius plot of calculated rate constants from the most accurate method considered here, namely CVT/SCT/HR (HR denotes hindered rotor), and available experimental data, is shown in Figure 3. First, treatment of the motions of the two methyl groups about the symmetry rotational axis as a hindered rotor rather than a harmonic oscillator decreases the rate constant as the temperature increases. In particular, it affects the rate only by 2% at room temperature but lowers the rate constants by 34% and 51% at 1000 and 2000 K, respectively. Table 3 also lists the tunneling transmission coefficients calculated using the one-dimensional Eckart, multidimensional zero-curvature ZCT, and small-curvature SCT methods. It is known that the Eckart function tends to produce a rather narrow potential width, resulting in overestimations in the tunneling contributions, particularly at low temperatures. This can be seen by comparing the Eckart tunneling factor of 282 with the SCT factor of 76 at 300 K. In the ZCT method, tunneling is assumed to be along the MEP whereas in the SCT method, due to the centrifugal force arising from the negative kinetic energy (in the tunneling regime), a tunneling path can cut the corner on the concave side of the MEP resulting in a shorter tunneling path. This corner cutting effect results in an enhancement in the tunneling probability. In fact, at 300 K, these effects increase the tunneling transmission coefficient by a factor of 4.12. The effects are smaller due to the smaller tunneling contribution as the temperature increases. The overall tunneling contribution as predicted by the SCT method is rather significant, particularly at the lower temperature range. In particular, at 500 K tunneling enhances the rate by a factor of 5.4 whereas it enhances the rate by a factor of 76 at 300 K. It is important to point out that the $CH_3 + CH_4 \rightarrow CH_4 + CH_3$ reaction belongs to the H-L-H (heavy-light-heavy) reaction type. And for such a reaction type it is known that due to the large curvature of the potential energy

TABLE 1: Optimized Geometries and Calculated Harmonic Frequencies of the Transition State of the $CH_3 + CH_4$ Reaction (distances are in Å and angles in deg; and numbers in parentheses are degeneracy)

	MP2/DZP* [b]	B3LYP/6-31G(2d)[c]	BH&HLYP/cc-pVDZ[a]	QCISD/cc-pVDZ[a]
C−H′	1.322	1.346	1.340	1.346
C−H	1.087	1.090	1.090	1.101
H−C−H′	105.0	105.4	105.4	105.5
ω (cm^{-1})	2008*i*, 76, 342(2), 546, 706(2), 1212, 1229, 1411(2), 1479(2), 1501(2), 3148, 3150, 3311(2), 3312(2)	1657*i*, 22, 331(2), 509, 711(2), 1178, 1207, 1398(2), 1470(2), 1492(2), 3084, 3085, 3212(2), 3213(2)	1884*i*, 43, 332(2), 522, 704(2), 1176, 200, 1378(2), 1462(2), 1485(2), 3142, 3144, 3286(2), 3287(2)	1923*i*, 47, 331(2), 519, 695(2), 1161, 1187, 1359(2), 1444(2), 1467(2), 3080, 3082, 3223(2), 3224(2)

[a] This work. [b] Reference 37. [c] Reference 38.

TABLE 2: Calculated Barrier Heights (kcal/mol) for the $CH_3 + CH_4$ Reaction

level of theory	$\Delta V^{\neq}$
B3LYP[b]	14.6
KMLYP[c]	14.8
G2[c]	18.5
CBS-APNO[c]	16.5
BH&HLYP[a]	17.4
QCISD[a]	19.0
PMP4//BH&HLYP[a]	18.0
CCSD(T)//BH&HLYP[a]	18.1
PMP2//UMP2[b]	16.4
CCSD(T)//UMP2[b]	17.6

[a] This work [b] Reference 39. [c] Reference 40.

surface along the reaction coordinate, the small curvature tunneling approximation tends to underestimate the tunneling contributions particularly at low temperatures, i.e., $T < 300$ K. To obtain more accurate tunneling contributions a large-curvature tunneling approximation would be required. However, such a method requires significantly more potential energy information and thus is not feasible with the level of electronic structure theory employed here. Furthermore, since we are interested only in the temperature range that is important for combustion, i.e., 300−2000 K, the SCT method would be sufficient. The comparison between our theoretical and experimental values is also shown in Figure 3. Our calculated rate constants at the most accurate level, i.e., CVT/SCT/HR, are in excellent agreement with experimentally derived values by Arthur et al.[7] and Dainton et al.,[8] though better with the former than the latter. The differences with those from Arthur et al. are typically less than a factor of 2. CVT/SCT/HR rate constants are fitted to an Arrhenius expression and are given by:

$$k_p = (6.20 \times 10^{-27}) T^{5.85} \exp(-5438.45/T) \quad (\text{cm}^3\ \text{molecule}^{-1}\ \text{s}^{-1})$$

3.2. $CH_3 + C_2H_6$ Reaction. The criteria of choosing the reference reaction for the RC-TST/LER is not limited to just the smallest reaction, specifically the $CH_3 + CH_4$ reaction (R1). Although the reaction of methane and methyl radical is the smallest reaction in which its rate constants can be calculated using an accurate dynamical and sufficiently high level of electronic structure theory as discussed above, it is known to have unique behaviors that differ from those of larger hydrocarbons due to its lack of a C−C bond. For instance, the barrier height of reaction R1 is noticeably larger than those of other reactions in the class by greater than 2 kcal/mol (as discussed below). Our previous study of another reaction class has shown that reaction R1 is not a good representative reaction to be used as the reference reaction for other hydrocarbons in the class. In fact, our analysis of both methane and ethane confirms this fact by showing that the ethane reaction gives a better correlation than the methane reaction, especially for the partition factors.

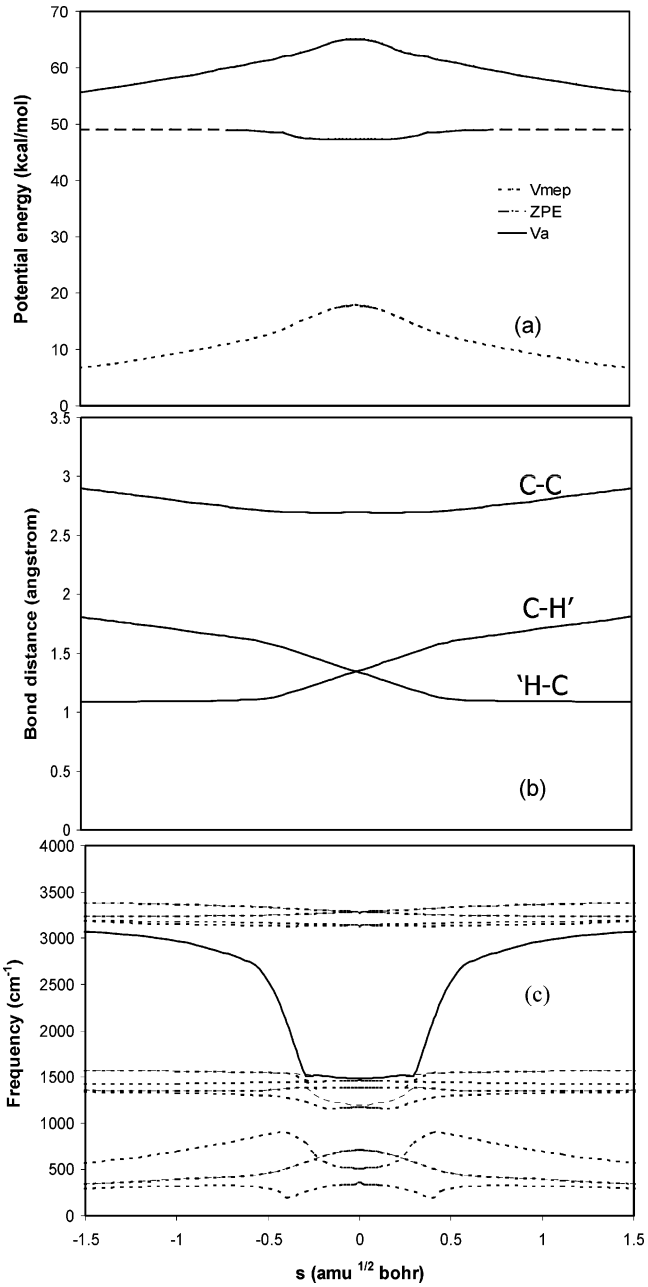

Figure 2. Potential engery profile (a), variations of selected bond lengths (b), and variations of the generalized vibrational frequencies (c) of the $CH_3 + CH_4$ reaction as functions of the reaction coordinate, *s*, at the BH&HLYP/cc-pVDZ level.

For these reasons, the parameters for the RC-TST/LER method are derived by the use of the reaction of methyl radical with ethane as the reference reaction. The results and discussions are shown in the section on parameters for the RC-TST/LER method below.

TABLE 3: Thermal Rate Constants $k(T)$ (cm^3 $molecule^{-1}$ s^{-1}) for the $CH_3 + CH_4 \rightarrow CH_3 + CH_4$ Reaction, Hindered Rotor (HR) Correction Factor, and Tunneling Corrections $\kappa(T)$

	$\kappa(T)$					$k(T)$		
T (K)	HR	Eckart	ZCT	SCT	CVT	CVT/SCT/HR	ref 7	ref 8
300	0.981	281.8	18.57	76.47	2.81×10^{-25}	2.21×10^{-23}		
350	0.947	41.07	8.31	26.64	2.01×10^{-23}	5.60×10^{-22}	9.14×10^{-22}	
400	0.914	13.87	4.96	13.09	5.14×10^{-22}	7.13×10^{-21}	1.24×10^{-20}	
450	0.884	7.27	3.48	7.90	6.60×10^{-21}	5.65×10^{-20}	9.44×10^{-20}	3.29×10^{-19}
500	0.856	4.82	2.70	5.44	5.24×10^{-20}	3.10×10^{-19}	4.78×10^{-19}	1.69×10^{-18}
550	0.829	3.65	2.24	4.10	2.93×10^{-19}	1.32×10^{-18}	1.80×10^{-18}	6.46×10^{-18}
600	0.805	2.99	1.94	3.20	1.26×10^{-19}	4.62×10^{-18}	5.45×10^{-18}	1.97×10^{-17}
800	0.725	1.95	1.40	1.94	8.11×10^{-17}	1.82×10^{-16}		
1000	0.663	1.61	1.20	1.50	1.17×10^{-15}	2.07×10^{-15}		
1500	0.557	1.32	1.04	1.16	6.02×10^{-14}	8.29×10^{-14}		
2000	0.490	1.21	1.00	1.06	5.77×10^{-13}	7.10×10^{-13}		
2500	0.442	1.16	0.98	1.02	2.65×10^{-12}	3.04×10^{-12}		

To use the $CH_3 + C_2H_6$ reaction as the reference reaction, its thermal rate constants are needed. This is done by carrying out the conventional TST rate calculation for the $CH_3 + C_2H_6$ reaction with explicit treatment of the methyl and ethyl internal rotations as hindered rotors. The barrier used in the rate calculation is the BH&HLYP barrier height of 15.84 kcal/mol scaled by the factor of 1.04. This factor was used to scale the BH&HLYP barrier of the $CH_3 + CH_4$ reaction to match the CCSD(T) result as discussed above. The tunneling contribution is obtained by scaling the κ^{SCT} of the $CH_3 + CH_4$ reaction by the scaling factor f_κ from eq 3. The resulting rate constants for the $CH_3 + C_2H_6$ reaction are given by:

$$k_{ref} = (2.47 \times 10^{-31})T^{6.04} \exp(-3039.5/T) \quad (cm^3\ molecule^{-1}\ s^{-1})$$

Figure 4 shows that our calculated rate constants compared well to available suggested data although there are no direct experimental values for this reaction.

3.3. Reaction Class Parameters. *Linear Energy Relationship* (*LER*). In our previous study,[6] we found that within a given reaction class there is a linear energy relationship between the reaction barriers and reaction energies similar to the Evans−Polanyi linear energy relationship.[22,23] These reaction energies can be calculated at a lower level of theory such as AM1.[24] Our aim here is to obtain the relationship between the barrier height and the reaction energy so that one only needs the reaction energy calculated by a relatively simple method to predict the thermal rate constant for a given reaction in the class without further calculations of the transition state geometry, energy, and frequencies. In our previous study,[25] we have shown that within the reaction class framework, an accurate relative barrier height can be obtained from a reasonably low level of theory such as DFT. To also illustrate this point here, we provide the relative barrier heights (listed in Table 4) calculated at the IMOMO(CCSD(T)/cc-pVTZ:BH&HLYP/cc-pVDZ) level, where the principal reaction is used as the model system, and at the BH&HLYP/cc-pVDZ level. The IMOMO method employed in combination with the reaction class concept has been shown to give rather accurate absolute classical barrier heights.[15] The relative barrier heights are also shown in Table 4. Note that BH&HLYP is able to predict the relative barrier heights in comparable accuracy with the IMOMO(CCSD(T):BH&HLYP) level to within a 0.3 kcal/mol difference except for reaction R13 the difference is 0.93 kcal/mol (differences of values in parentheses in columns 4 and 5 of Table 4). For the principal reaction, the reaction barrier height calculated at BH&HLYP/cc-pVDZ is corrected to the reaction barrier height calculated at the CCSD(T)/cc-pVTZ level. The relationships for all reactions including primary, secondary, and tertiary hydrogen abstraction reactions were fitted to the following expressions.

$$\Delta V^{\neq} = -0.3446\Delta E + 18.001 \text{ (kcal/mol)} \quad (\Delta E \text{ from AM1 calculations}) \quad (7a)$$

$$\Delta V^{\neq} = -0.5568\Delta E + 18.138 \text{ (kcal/mol)} \quad (\Delta E \text{ from BH\&HLYP calculations}) \quad (7b)$$

The standard deviations are 0.21 and 0.20 kcal/mol for expressions 7a and 7b, respectively. A large degree of linearity of the

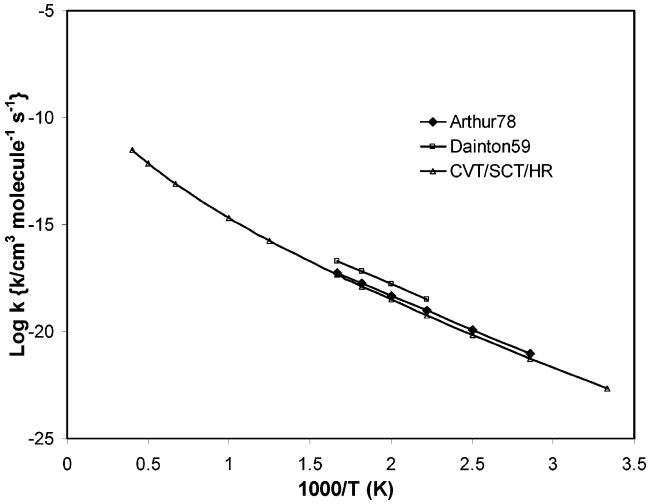

Figure 3. Arrhenius plot of the calculated and available experimental data rate constants for the $CH_3 + CH_4$ reaction.

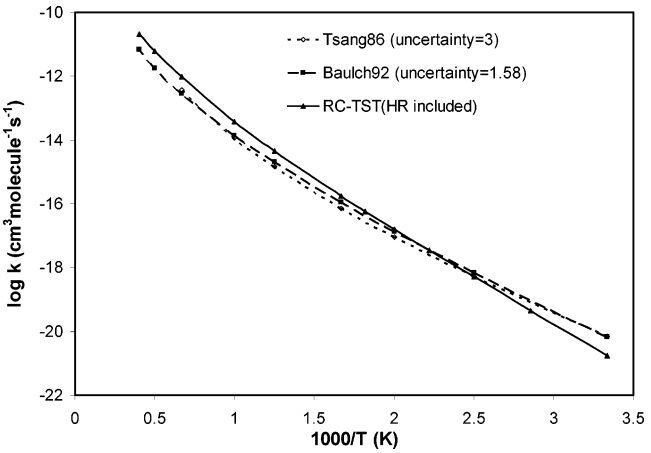

Figure 4. Arrhenius plot of the calculated and available experimental data rate constants for the $CH_3 + C_2H_6$ reaction. Numbers in parentheses are uncertainty values which are taken from the NIST kinetics database.[41]

TABLE 4: Reaction Barriers ($\Delta V^{\neq}$), Reaction Energies (ΔE), and Deviations (kcal/mol)

reaction	ΔE^a	ΔE^b	$\Delta V^{\neq\,c}$	$\Delta V^{\neq\,d}$	$\Delta V^{\neq}{}_{\mathrm{LER}}{}^e$	$\lvert \Delta V^{\neq} - \Delta V^{\neq}{}_{\mathrm{LER}} \rvert$ [f]
R1	0.00	0.00	17.41 (0.00)	18.14 (0.00)	18.00	0.14
R2	4.12	5.84	15.19 (2.22)	15.84 (2.29)	15.98	0.14
R3	3.27	5.65	15.49 (1.92)	16.32 (1.82)	16.04	0.28
R4	7.39	11.04	13.37 (4.04)	14.02 (4.12)	14.17	0.15
R5	3.79	5.71	15.40 (2.01)	16.02 (2.11)	16.02	0.00
R6	7.07	10.86	13.63 (3.78)	14.20 (3.94)	14.24	0.04
R7	3.32	5.15	15.65 (1.76)	16.29 (1.85)	16.22	0.07
R8	9.26	15.50	11.85 (5.56)	12.98 (5.16)	12.63	(0.35)[h]
R9	3.79	5.65	15.37 (2.04)	16.03 (2.11)	16.04	0.01
R10	7.14	10.86	13.58 (3.83)	14.16 (3.98)	14.24	0.08
R11	6.77	10.48	13.99 (3.42)	14.37 (3.77)	14.37	0.00
R12	2.77	4.23	15.99 (1.42)	16.59 (1.54)	16.54	0.05
R13	4.35	5.84	15.92 (1.49)	15.71 (2.42)	15.98	0.27
R14	7.08	10.42	13.82 (3.59)	14.19 (3.94)	14.39	0.20
R15	9.29	15.25	12.55 (4.86)	12.96 (5.17)	12.72	0.24
R16	3.41	5.08	15.68(1.73)	16.24(1.90)	16.24	0.00
MAD						0.13[g]

[a] Calculated at the BH&HLYP/cc-pVDZ level of theory. [b] Calculated at the AM1 level of theory. [c] Calculated at the BH&HLYP/cc-pVDZ level of theory; the numbers in parentheses are the relative barrier heights. [d] Calculated at the IMOMO(CCSD(T)//cc-pVTZ:BH&HLYP/cc-pVDZ) level of theory as described in the text; the numbers in parentheses are the relative barrier heights. [e] Calculated from LER by substituting AM1 reaction energies into eq 7. [f] $\Delta V^{\neq}$ IMOMO(CCSD(T)/cc-pVTZ:BH&HLYP/cc-cVDZ) barrier; $\Delta V^{\neq}{}_{\mathrm{LER}}$ reaction barrier height from LER/AM1. [g] Mean absolute deviations for reactions R1−R16. [h] Max absolute deviation of all reactions R1−R16.

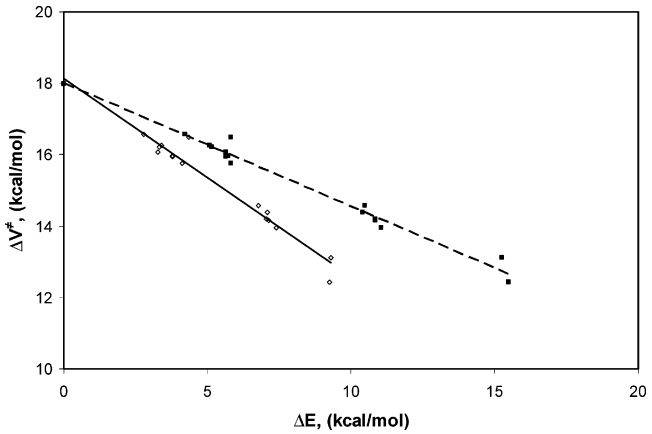

Figure 5. Linear energy relationships between reaction energy (ΔE) and reaction barrier height ($\Delta V^{\neq}$). ΔE values were calculated at the BH&HLYP/cc-pVDZ (square symbols and dashed line) and AM1 levels of theory (diamond symbols and solid line). Barrier heights were calculated at the IMOMO (CCSD(T)/cc-pVTZ:BH&HLYP/cc-pVDZ) level of theory.

LERs over the entire reaction energy range considered here is due partly to the small range of barrier heights, namely from 13 to 18 kcal/mol. Note that these LER relationships are universal to all reactions in the class and do not depend on a specific reaction chosen as the reference reaction in the RC-TST method. Figure 5 shows the linear energy relationships between reaction barrier heights calculated at the IMOMO-(CCSD(T)/cc-pVTZ:BH&HLYP/cc-pVDZ) level of theory and reaction energies calculated at BH&HLYP and AM1 levels of theory, respectively. The calculated reaction energies, reaction barrier heights, and absolute deviations between calculated barrier heights from LER and those from full quantum calculations are listed in Table 4. It can be seen that the average absolute deviations for the reaction barrier height between LER and IMOMO(CCSD(T)/cc-pVTZ:BH&HLYP/cc-pVDZ) calculation are smaller than 1 kcal/mol. The averaged deviation of reaction barrier heights predicted from AM1 reaction energy using LER is 0.13 kcal/mol for all reactions. These deviations are in fact smaller than the systematic errors of the computed absolute classical barriers from electronic structure calculation.

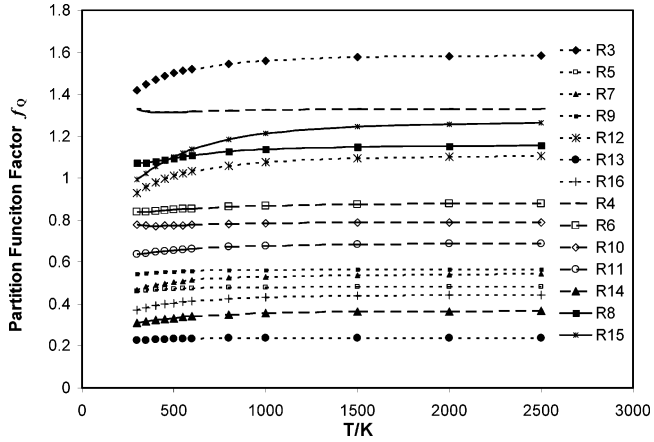

Figure 6. Plot of partition function factors f_Q as functions of the temperature for reactions R3−R16: primary carbon (dot line), secondary carbon (dash line), and tertiary carbon (solid line).

Partition Function Factor. In our previous study,[6] we have discussed that f_Q results mainly from the difference in coupling between the substituents and the reactive moiety of the considered reaction and the reference reaction. In calculations of f_Q, vibrational frequencies calculated at the BH&HLYP level were used. Also since the $CH_3 + C_2H_6$ reaction was used as the reference reaction, hindered rotor treatments for the methyl and ethyl groups were explicitly included in the reference rate constants. Figure 6 shows the temperature dependence of f_Q for different types of hydrogen atom and the f_Q varies narrowly from 0.2 to 1.6 and again for simplicity we approximate f_Q to be 0.5, 0.8, and 1.1 for primary, secondary, and tertiary hydrogen, respectively. This would make the largest error on the average in f_Q of only about 40% with the exception of reaction R3, which has an error factor of 3. This is certainly an acceptable level of accuracy in kinetics modeling. One could further introduce the temperature dependence into f_Q at the lower temperature range; however, we found that it would only reduce the error in f_Q slightly.

Calculation of Symmetry Number Factor. The symmetry number factors were simply derived from the ratio of symmetry numbers of target and principal reactions using reaction R2 as a reference reaction.

Calculation of Tunneling Factor. We use the Eckart tunneling method[26] to calculate the tunneling factor, which is the ratio of tunneling coefficients for the target and reference reactions. This method requires only the imaginary frequency and forward and reverse barrier height of the reaction. Table 5 shows the calculated tunneling factors of reactions in the class using barrier heights calculated from the BH&HLYP level for reaction R2 as a reference reaction. Since all reactions in the class are exothermic except the principal reaction, the forward barriers heights dominate the quantum tunneling effect. At a given temperature, the f_κ values of the abstraction reactions for the same type of hydrogen atom are plotted in Figure 7. For reaction R2 as a reference reaction, the fitted equations for abstraction of hydrogen from a primary, secondary, and tertiary carbon are $f_\kappa(T) = 1/(-43.58 + 44T^{0.002})$ for primary carbon, $f_\kappa(T) = 1.040-(1 - e^{-0.003T})$ for secondary carbon, and $f_\kappa(T) = 1.080(1 - e^{-0.001T})$ for tertiary carbon, respectively.

TABLE 5: Calculated Symmetry Number Factors and Tunneling Factors at 300 K (using reaction R2 as the reference reaction)

reaction	f_σ	f_κ
R2	1.00 (6)[a]	1.00 (85)[a]
R3	1.00	1.29
R4	0.33	0.28
R5	1.00	1.11
R6	0.67	0.33
R7	1.50	1.29
R8	0.17	0.08
R9	1.00	1.11
R10	0.67	0.33
R11	0.33	0.40
R12	2.00	1.58
R13	0.50	1.25
R14	0.33	0.36
R15	0.17	0.10
R16	1.00	1.29

[a] Values in parentheses are the absolute symmetry and tunneling coefficient.

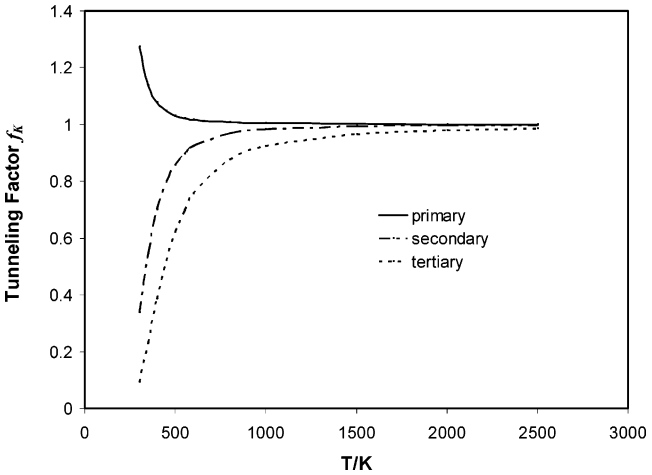

Figure 7. Plot of the tunneling factor f_κ with temperature for hydrogen abstract reactions on primary carbon (solid line), secondary carbon (long dashed line), and tertiary carbon (dotted line).

Calculation of Potential Factor. The potential energy factor f_V can be calculated using eq 6, where $\Delta\Delta V^{\neq}$ is the difference in the classical reaction barriers of target reaction and reference reaction. The LERs discussed above are used for estimating the barrier height for the target reaction from its reaction energy.

Hindered Rotor Correction Factor. It is important to point out that the motion of the internal rotation of the methyl group in the reactive moiety is already treated explicitly in the rate constants of the reference $CH_3 + C_2H_6$ reaction. Here we examine the correction factor for internal rotations of the substituent groups. In this study, the HR correction factor was computed using the same method as in the work of Ayala et al.[21] The absolute HR correction factors for 1, 2, and 3 methyl groups as in the $CH_3 + H_3CCH_3$ (R2), $CH_3 + H_3CCH_2CH_3 \rightarrow CH_4 + H_3CCHCH_3$ (R4), and $CH_3 + HC(CH_3)_3 \rightarrow CH_4 + C(CH_3)_3$ (R8) reactions are shown in Table 6 and plotted in Figure 8. It can be seen from Figure 8 that the HR correction factors are dependent on the temperature. From Table 6, the ratios of the representative reactions R4 and R8 (for 2 and 3 methyl groups) to the reference reaction R2 (for 1 methyl group) show that the effects of HR due to substituent groups are small as these relative factors are close to unity for the entire temperature range. For this reason, we can reasonably assume that the effects of the internal rotations of the substituent groups

TABLE 6: Calculated Hinder Rotation Correction Factors to the Rate Constant for 1 and 2 and 3 Methyl Groups in the Transition State (calculated from reactions R2, R4, and R8, respectively)

	hinder of rotation correction factors		
T (K)	1 methyl	2 methyls	3 methyls
300	1.15	1.15	1.17
350	1.15	1.13	1.16
400	1.14	1.10	1.14
450	1.12	1.08	1.12
500	1.10	1.06	1.09
550	1.09	1.04	1.07
600	1.07	1.02	1.05
800	1.02	0.97	0.97
1000	0.98	0.93	0.91
1500	0.89	0.84	0.80
2000	0.79	0.78	0.73
2500	0.70	0.68	0.68

are canceled out in the RC-TST theory particularly for this reaction class with the use of reaction R2 as the reference reaction. This observation, however, may not be true in general and thus it should be investigated for each reaction class. In fact, we found that such effects are not negligible in another reaction class.[27]

Prediction of Rate Constants. We now can predict the rate constants for all reactions in the class after we have established the LER between the reaction barrier height and reaction energy, as well as knowing the partition function factor, symmetry number factor, tunneling factor, and potential energy factor using reaction R2 as the reference reaction by following this procedure: (1) calculate f_σ from symmetry numbers of the target and reference reactions using eq 5; (2) assign f_Q to be 0.5, 0.8, or 1.1 for abstraction of hydrogen from primary, secondary, or tertiary carbon, respectively; (3) calculate f_κ from eqs 8−10 according to the type of hydrogen abstraction; and (4) calculate the reaction barrier height using the LERs shown in eq 7a or 7b depending on how the reaction energy was calculated at the AM1 or BH&HLYP level of theory. f_V is then calculated from eq 6 using the barrier height of the reference reaction of 15.84 kcal/mol. Table 7 summarizes the RC-TST parameters for this reaction class with reaction R2 as the reference reaction. We selected several reactions whose rate constants were available experimentally or derived from other experimental data for more detailed discussion to illustrate the theory.

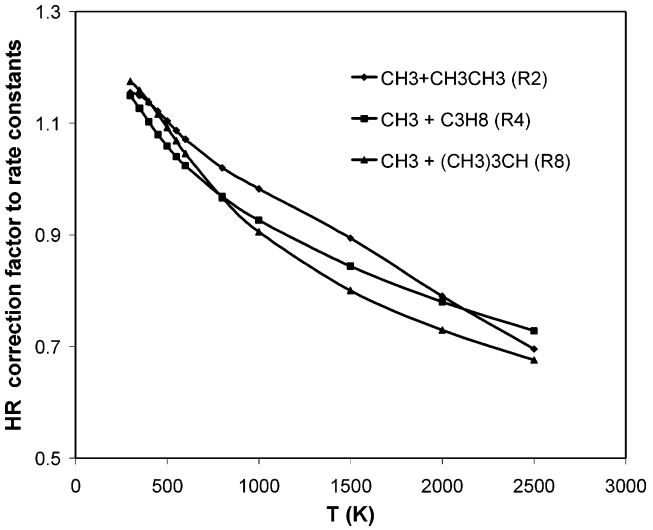

Figure 8. Plot of hindered rotation correction factors versus the temperature for 1, 2, and 3 methyl groups (which are represented by reactions R2, R4, and R8, respectively).

TABLE 7: Ab Initio Derived Parameters and Formulation of the RC-TST/LER Method for the CH_3 + Alkane Hydrogen Abstraction Reaction Class

$k(T) = f_\kappa(T) f_\sigma f_Q(T) f_V(T)$; $f_V(T) = \exp\{-(\Delta V^{\neq} - \Delta V^{\neq}_p)/k_B T\}$	
	$CH_3 + C_2H_6$ as the reference reaction
$f_\kappa(T)$	$1/(-43.58 + 44T^{0.002})$ for primary carbon $1.040(1 - e^{-0.003T})$ for secondary carbon $1.080(1 - e^{-0.001T})$ for tertiary carbon
f_Q	0.5 (primary), 0.8 (secondary), and 1.1 (tertiary)
$\Delta V^{\neq}$ (kcal/mol)	$(-0.5568\Delta E + 18.138)$ for all types, ΔE at the BH&HLYP/cc-pVDZ level $(-0.3446\Delta E + 18.001)$ for all types, ΔE at the AM1 level
$\Delta V^{\neq}_p$ (kcal/mol)	15.84
$k_{ref}(T)$	$(2.47 \times 10^{-31}) T^{6.04} \exp(-3039.5/T)$ (cm^3 $molecule^{-1}$ s^{-1})

Figure 9a,b shows the predicted rate constants of reaction R4 and reaction R8 using the RC-TST/LER method and the suggested rate constants.[28−35] These reactions represent hydrogen abstraction from a secondary and tertiary carbon, respectively. The agreement between our predicted results and those suggested from literature reviews or derived from other experimental data is reasonable for these two reactions. These comparisons, however, do not reflect the accuracy of the RC-TST/LER method. Such error analyses are given below.

Error Analyses. To estimate the overall efficiency of the RC-TST/LER method, we performed two different error analyses. First, we compared the calculated rate constants for a selected number of reactions using both the RC-TST/LER and full conventional TST/Eckart methods. Second, we examined the errors in different factors in the RC-TST/LER method. In particular, errors in f_κ are from the assumption of the same value for the same type of abstracting hydrogen. Errors in f_Q are from using a constant for all reactions in the class. Errors in f_V are from using the LER expression.

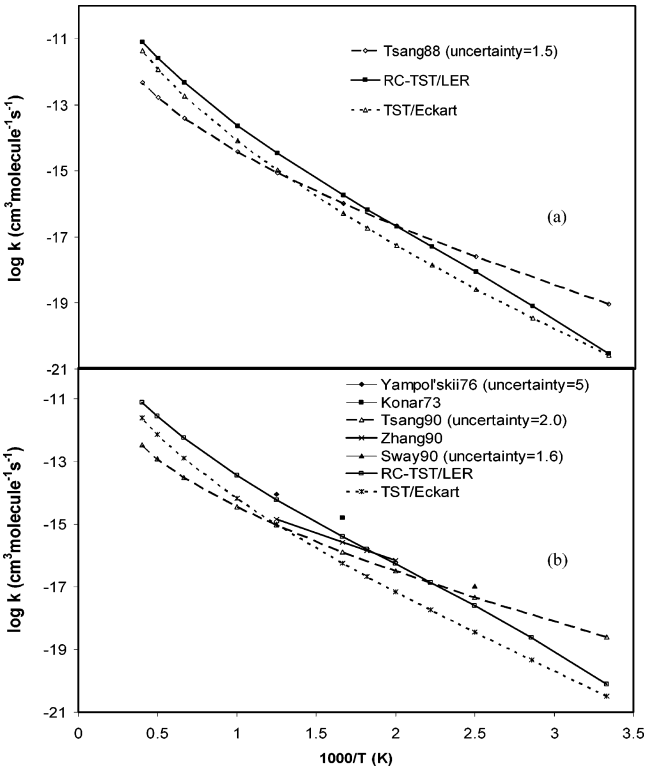

Figure 9. Arrhenius plots of the calculated rate constants using the RC-TST/LER method for some representative reaction along with the available literature values as well as the calculated TST/Eckart rate constants: (a) $CH_3 + C_3H_8$ (secondary carbon) and (b) $CH_3 + (CH_3)_3$-CH (tertiary carbon).

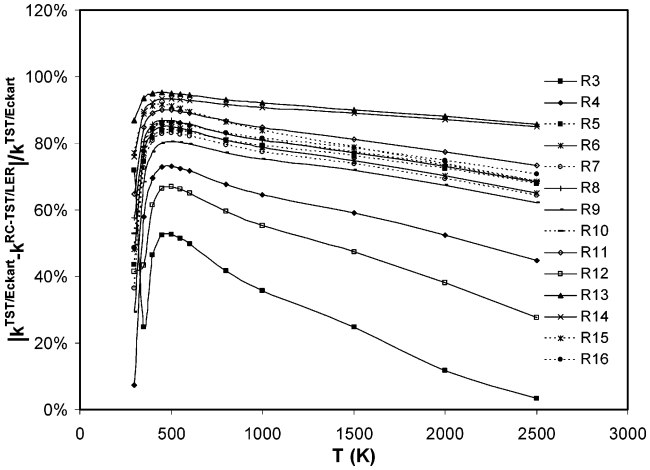

Figure 10. Relative deviations as functions of the temperature between rate constants calculated from the RC-TST/LER and explicit TST/Eckart methods.

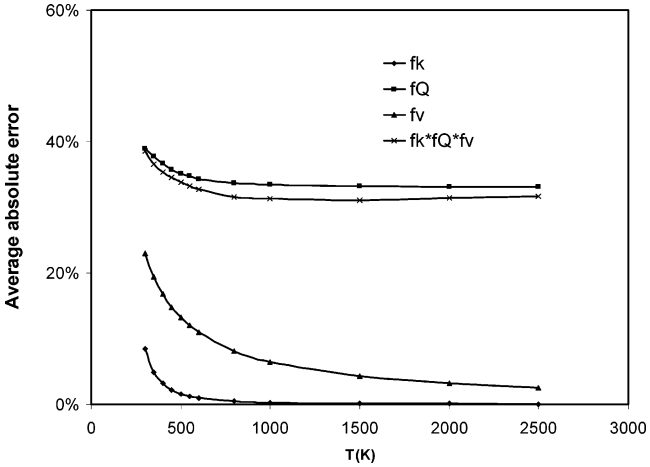

Figure 11. Average absolute errors of the total relative rate factor $f(T)$ (eq 3) and its components, namely the tunneling (f_κ), partition (f_Q), and potential (f_V) factors as functions of the temperature.

The results from the first analysis are showed in Figure 10. Here we plotted the relative deviation defined by $(|k^{TST/Eckart} - k^{RC-TST/LER}|/k^{RC-TST/LER})$ percent versus the temperature for reactions R3−R16. The relative errors are less than 100% for all reactions. This is certainly an acceptable level of accuracy for reaction engineering purposes. It should be noted that this analysis is not precise since the RC-TST/LER is an extrapolation of the CVT/SCT method as it was used to calculate rate constants for the $CH_3 + CH_4$ reaction not the TST/Eckart. Thus, one can expect larger differences when comparing the RC-TST/LER results to those from full TST/Eckart.

The results of the second analysis on the errors from different relative rate factors, namely f_κ, f_Q, and f_V, used in the RC-TST/LER method are shown in Figure 11. We plotted the absolute errors averaged for reactions R3−R16. The errors in the relative rate factors provide measures for the errors introduced by using simple expressions for the tunneling factors and partition function factors, and the use of the LER's for estimating the potential energy factors. Note that the symmetry factor is exact. The total error is the product of individual error factors. Errors from all components are less than 40% for the temperature range from 300 to 2500 K. The tendency of errors decreases as the temperature increases. The total errors in the relative rate factors

are also less than 40% and decrease as the temperature increases. These are systematic errors of the RC-TST/LER method that can be compared with the results reported by Green et al.[36] using the TST/Wiger to predict the rate constants of the reaction using the group additivity approach. We found that both methods have similar systematic errors. The main difference is that the RC-TST/LER method approximates the CVT/SCT/hinder level of theory, whereas the GA method approximates only the TST/Wigner level. It is well-known that the multidimensional semiclassical small curvature tunneling (SCT) method is much more accurate on predicting the tunneling coefficient than the simple Wigner method particularly for reactions of the H-L-H type.

4. Conclusions

We have studied the dynamics and temperature dependence of rate constants for the hydrogen abstraction $^{\bullet}CH_3 + CH_4 \rightarrow CH_4 + {}^{\bullet}CH_3$. The theoretical rate constants in the temperature range 300−2500 K are obtained by CVT with ZCT, SCT, and hindered rotor. The calculated rate constants are in good agreement with available experimental values over the measured temperature range. Our results show that the tunneling correction plays a critical role in the lower temperature range whereas effects of hindered rotations are more important at high temperatures. We have extended our application of the reaction class transition state theory combined with the linear energy relationship (RC-TST/LER) to the prediction of thermal rate constants for hydrogen abstraction reactions of the $^{\bullet}CH_3$ + alkane class. The RC-TST/LER is found to be a promising method for predicting rate constants for a large number of reactions in a given reaction class. Our analyses indicate that less than 40% systematic errors on the average exist in the predicted rate constants using the RC-TST/LER method while comparing to explicit rate calculations the differences are less than 100% or a factor of 2 on the average, thus this method would be useful for estimates of rate constants for reactions involved in complex combustion systems such as combustion of hydrocarbons.

Acknowledgment. This work is supported in part by the National Science Foundation. N.K. is grateful to the Royal Thai Embassy for a Graduate Fellowship. The authors would like to thank the University of Utah Center for High Performance Computing for computer resources and support.

Note Added after ASAP Publication. This article was released ASAP on August 5, 2005. Data in column 3 of Table 4 has been revised. The correct version was posted on August 11, 2005.

References and Notes

(1) Goos, E.; Hippler, H.; Hoyermann, K.; Jurges, B. *Int. J. Chem. Kinet.* **2001**, *33*, 732.
(2) Chandra, A. K.; Rao, V. S. *Int. J. Quantum Chem.* **1993**, *47*, 437.
(3) Leroy, G.; Sana, M.; Tinant, A. *Can. J. Chem.* **1985**, *63*, 1447.
(4) Susnow, R. G.; Dean, A. M.; Green, W. H., Jr. *Chem. Phys. Lett.* **1999**, *312*, 262.
(5) Truong, T. N. *J. Chem. Phys.* **2000**, *113*, 4957.
(6) Zhang, S.; Truong, T. N. *J. Phys. Chem. A.* **2003**, *107*, 1138.
(7) Arthur, N. L.; Bell, T. N. *Rev. Chem. Intermed.* **1978**, *2*, 37.
(8) Dainton, F. S.; Ivin, K. J.; Wilkinson, F. *Trans. Faraday Soc.* **1959**, *55*, 929.
(9) Steacie, E. W. R. *Atomic and Free Radical Reactions*; Reinhold: New York, 1954.
(10) Frisch, M. J.; Trucks, G. W.; Schlegel, H. B.; Scuseria, G. E.; Robb, M. A.; Cheeseman, J. R.; Zakrzewski, V. G.; Montgomery, J. A., Jr.; Stratmann, R. E.; Burant, J. C.; Dapprich, S.; Millam, J. M.; Daniels, A. D.; Kudin, K. N.; Strain, M. C.; Farkas, O.; Tomasi, J.; Barone, V.; Cossi, M.; Cammi, R.; Mennucci, B.; Pomelli, C.; Adamo, C.; Clifford, S.; Ochterski, J.; Petersson, G. A.; Ayala, P. Y.; Cui, Q.; Morokuma, K.; Malick, D. K.; Rabuck, A. D.; Raghavachari, K.; Foresman, J. B.; Cioslowski, J.; Ortiz, J. V.; Baboul, A. G.; Stefanov, B. B.; Liu, G.; Liashenko, A.; Piskorz, P.; Komaromi, I.; Gomperts, R.; Martin, R. L.; Fox, D. J.; Keith, T.; Al-Laham, M. A.; Peng, C. Y.; Nanayakkara, A.; Gonzalez, C.; Challacombe, M.; Gill, P. M. W.; Johnson, B.; Chen, W.; Wong, M. W.; Andres, J. L.; Gonzalez, C.; Head-Gordon, M.; Replogle, E. S.; Pople, J. A. *Gaussian 03*, Revision A.7; Gaussian, Inc.: Pittsburgh, PA, 1998.
(11) Lynch, B. J.; Fast, P. L.; Harris, M.; Truhlar, D. G. *J. Phys. Chem. A* **2000**, *104*, 4811.
(12) Zhang, Q.; Bell, R.; Truong, T. N. *J. Phys. Chem.* **1995**, *99*, 592.
(13) Truong, T. N.; Duncan, W. *J. Chem. Phys.* **1994**, *101*, 7408.
(14) Gonzalez, C.; Schlegel, H. B. *J. Phys. Chem.* **1990**, *94*, 5523.
(15) Truong, T. N.; Truong, T.-T. T. *Chem. Phys. Lett.* **1999**, *314*, 529.
(16) Svensson, M.; Humbel, S.; Morokuma, K. *J. Chem. Phys.* **1996**, *105*, 3654.
(17) Humbel, S.; Sieber, S.; Morokuma, K. *J. Chem. Phys.* **1996**, *105*, 1959.
(18) Truong, T. N. http://cseo.net.
(19) Truhlar, D. G.; Isaacson, A. D.; Skodje, R. T.; Garrett, B. C. *J. Phys. Chem.* **1982**, *86*, 2252.
(20) Truhlar, D. G. *J. Comput. Chem.* **1991**, *12*, 266.
(21) Ayala, P. Y.; Schlegel, H. B. *J. Chem. Phys.* **1998**, *108*, 2314.
(22) Evans, M. G.; Polanyi, M. *Proc. R. Soc. London, Ser. A* **1936**, *154*, 133.
(23) Polanyi, J. C. *Acc. Chem. Res.* **1972**, *5*, 161.
(24) Dewar, M. J. S.; Zoebisch, E. G.; Healy, E. F.; Stewart, J. J. P. *J. Am. Chem. Soc.* **1985**, *107*, 3902.
(25) Truong, T. N.; Maity, D. K.; Truong, T.-T. T. *J. Chem. Phys.* **2000**, *112*, 24.
(26) Miller, W. H. *J. Am. Chem. Soc.* **1979**, *101*, 6810.
(27) Huynh, K. L.; Truong, T. N. Kinetics of Hydrogen Abstraction by Hydroxyl Radical OH + Alkanes Reaction Class: An Application of the Reaction Class Transition State Theory. *J. Phys. Chem. A.* Submitted for publication.
(28) Sway, M. I. *Indian J. Chem., Sect. A* **1990**, *29A*, 748.
(29) Yampol'skii, Y. P.; Tsikhlinski, V. *Neftekhimiya* **1976**, *16*, 560.
(30) Baulch, D. L.; Cobos, C. J.; Cox, R. A.; Esser, C.; Frank, P.; et al. *J. Phys. Chem. Ref. Data* **1992**, *21*, 411.
(31) Tsang, W.; Hampson, R. F. *J. Phys. Chem. Ref. Data* **1986**, *15*, 1087.
(32) Tsang, W. *J. Phys. Chem. Ref. Data* **1988**, *17*, 887.
(33) Tsang, W. *J. Phys. Chem. Ref. Data* **1990**, *19*, 1.
(34) Konar, R. S.; Marshall, R. M.; Purnell, J. H. *Int. J. Chem. Kinet.* **1973**, *5*, 1007.
(35) Zhang, H. X.; Back, M. H. *Int. J. Chem. Kinet.* **1990**, *22*, 537.
(36) Sumathi, R.; Carstensen, H. H.; Green, W. H., Jr. *J. Phys. Chem. A* **2001**, *105*, 6910.
(37) Litwinowicz, J. A.; Ewing, D. W.; Jurisevic, S.; Manka, M. J. *J. Phys. Chem.* **1995**, *99*, 9709.
(38) Skokov, S.; Wheeler, R. A. *Chem. Phys. Lett.* **1997**, *271*, 251.
(39) Basch, H.; Hoz, S. *J. Phys. Chem. A* **1997**, *101*, 4416.
(40) Kang, J. K.; Musgrave, C. B. *J. Chem. Phys.* **2001**, *115*, 11040.
(41) NIST. http://kinetics.nist.gov.